J|A|C|S COMMUNICATIONS

Published on Web 02/01/2010

The Interfacial Tension of Nanoscopic Oil Droplets in Water Is Hardly Affected by SDS Surfactant

Hilton B. de Aguiar, Alex G. F. de Beer, Matthew L. Strader, and Sylvie Roke*

Max Planck Institute for Metals Research, Heisenbergstrasse 3, 70569 Stuttgart, Germany

Received November 9, 2009; E-mail: roke@mf.mpg.de

The properties of emulsions consisting of nanoscopic oil droplets dispersed in water are primarily determined by the local chemical environment (i.e., molecular structure and charge) of their interfaces.[1] In a detergent-containing emulsion the droplet interface is generally perceived as an interface with a high density of surfactant molecules. This view originates primarily from extrapolating experimental findings at planar interfaces.[1] In a common planar oil/water system such as bulk *n*-hexadecane in contact with bulk water, the surfactant sodiumdodecylsulfate (SDS) will reduce the interfacial tension from 52 mN/m to 10 mN/m by populating the interface.[2b−f,3] The apolar SDS tail resides in the oil phase, and the polar sulfate head group is immersed in the water.[2] At SDS concentrations approaching the critical micelle concentration (cmc) of 8 mM the interface is fully occupied by SDS molecules[3] giving rise to a surface coverage of 3.3×10^{-6} mol/m^2 (corresponding to an occupied molecular interfacial area of ∼40−50 Å^2). It is widely assumed[1a,b] that similar behavior can be expected for SDS adsorption on submicrometer sized *n*-hexadecane oil droplets dispersed in water.

Such nanoscopic droplets are too small for direct interfacial tension measurements. As was pioneered by the Eisenthal group,[4] the (electronic) structure of the interface can be probed with second harmonic scattering (SHS).[5] The SHS signal depends quadratically on the molecular surface density (N_s) and can be used to retrieve the interfacial energetics and population.[4b]

Here, we selectively probe the interfacial SDS molecules using vibrational sum frequency scattering (SFS)[6] on SDS-stabilized *n*-hexadecane ($C_{16}D_{34}$) droplets dispersed in D_2O. We have followed the adsorption of SDS onto oil droplets with a constant average radius of 83 nm, dispersed in D_2O. Stable 1 v.v.% emulsions were prepared with varying total SDS concentrations ($c_{tot,SDS}$) from 55 μM up to 10 mM (see the Supporting Information (SI) for creaming rates, Ostwald ripening data, and droplet size distribution). Since SDS molecules can either reside in the solution (with concentration c) or at the surface, we have $c_{tot,SDS} = N_sA/V + c$, where A is the total surface area (obtained from DLS) and V is the sample volume.

The vibrational SFS measurements were performed by shining an infrared (IR) and a visible (VIS) laser pulse[7] through an emulsion (Figure 1A). The p-polarized broadband IR field (tuned around 1100 cm^{-1}) can excite the IR dipole moment of the symmetric SO_3 stretch mode. Only the sulfate head groups in the first molecular layer around the droplet interface can, upon interaction with the narrowband s-polarized VIS field, simultaneously undergo a change in their electronic charge distribution. This second-order sum frequency (SF) polarization can emit a sum frequency photon.[8] Thus, SF photons are generated only by the SDS molecules at the oil/water interface of the droplet. Coherent interference on the droplet surface will give rise to a scattering pattern, which is peaked around a scattering angle (θ) of 60° with respect to the phase-matched direction of the incoming beams.

Figure 1B displays several SFS spectra recorded at this angle in ssp polarization. The SFS spectra can be described by scattering theory[6,8] and fit with a SO_3 symmetric stretch resonance[9a,b] centered at 1080 cm^{-1} with a constant line width for all SDS concentrations (15 cm^{-1}). The obtained amplitudes for both ppp (the spectra can be found in the SI) and ssp spectra are plotted in Figure 1C. It shows that a change in total SDS concentration of 2 orders of magnitude is accompanied by a change in SF amplitude of only a factor of 3.5. The signal for sps and pss polarization combinations was below our detection limit.

The SFS amplitude is determined by the orientation of the molecules, the local refractive index at the droplet interface, and the changing molecular interfacial density. Since we are working at a very small refractive index difference (0.1), with small droplet radii, and at very low surfactant concentrations, a change in Fresnel factors as the origin of the concentration-dependent amplitude change can be neglected. Changes in Fresnel factors would result in variations of the ssp/ppp intensity ratio (not observed; see Figure 1C), which is also true for changing orientation. These observations indicate that the amplitudes of the SFS signals are directly proportional to SDS surface density.

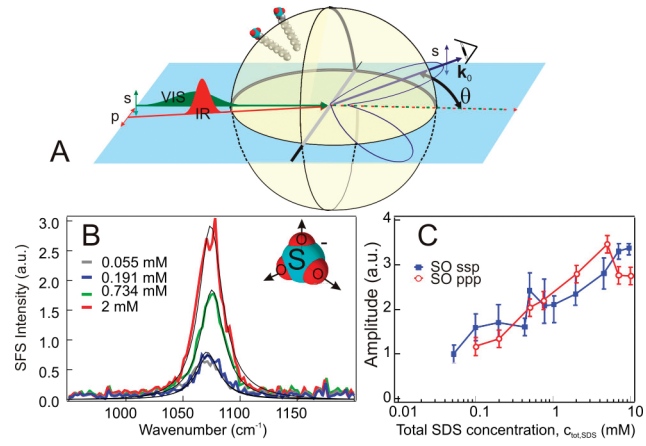

Figure 1. Sum frequency scattering (SFS) spectroscopy to measure the adsorption of SDS molecules on the oil/water droplet interface. (A) Illustration of the experiment in which p-polarized IR and s-polarized VIS beams generate s-polarized SF photons. (B) ssp-SFS spectra with fits obtained from the sulfate head groups located on the droplet interface for various total concentrations of SDS ($c_{tot,SDS}$). The droplet size distribution is constant for all SDS concentrations. (C) The resultant amplitudes of the symmetric SO_3 stretch mode for SFS spectra in ssp and ppp polarization plotted against the total SDS concentration.

Control experiments with a 8 mM solution of only SDS in D_2O gave no observable signal. SFS spectra of the SDS alkyl chains (see SI) show similar results: A modest, parallel intensity increase in both ssp and ppp polarization combination channels, with no indications of conformation changes of the alkyl chains. This

10.1021/ja9095158

observation supports the conclusion that the amplitude should relate linearly to the surface excess on the droplet interface.

Using the modified Langmuir model published by Wang et al.,[4b] in combination with the boundary condition that the surface density cannot exceed the total amount in solution (i.e., $A^*Ns \leq c_{tot,SDS}^*V$) and the known total droplet surface area, we can estimate the change in interfacial density (see the SI). The result is shown in Figure 2A. From the fit (blue line) we obtain an *upper limit* of 3.92×10^{-7}mol/m^2 for the saturation surface coverage (N_s^{max}) and -29.10 ± 0.58 kJ/mol for the Gibbs free energy of adsorption (ΔG). This corresponds to a *minimum* interfacial area of 425 Å^2 per SDS molecule as opposed to ~40−50 Å^2 for the planar interface. Evidently, there is an enormous difference between the adsorption behavior on a small *n*-hexadecane droplet and that on a planar interface. We have also observed similar behavior for other ionic surfactants.

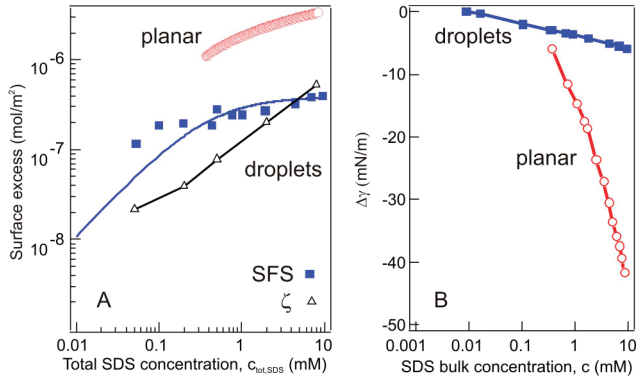

Figure 2. Planar vs droplet interface. (A) Surface excess (N_s) of SDS on a planar *n*-hexadecane/water interface (red circles, obtained from surface tension data), surface excess of SDS on *n*-hexadecane droplets in water (blue squares) obtained from the SFS amplitudes of the SFS data, and charge density induced by SDS on *n*-hexadecane droplets in water derived from ζ-potential data. The solid blue line is a fit to the modified Langmuir adsorption model.[4b] (B) The change in interfacial tension ($\Delta\gamma$) measured for a planar interface (red circles, see e.g. ref 3) and calculated from the surface excess of panel A (blue squares, using eq 1) as a function of SDS concentration in the liquid (c).

The retrieved upper limit for the number of SDS molecules at the surface can be compared with surface charge density data (Figure 2A, black triangles), obtained from a numerical model that we have applied to our ζ-potential measurements[1a,b,d] (see the SI). It can be seen that both densities are of the same order of magnitude as the charge density, so that both methods are in agreement with one another. Since both methods measure different species (uncharged sulfate groups vs negative charge), and because the ionic strength of the solution is very low (which makes it difficult to predict at what distance from the surface the ζ potential is measured), a more precise comparison is not possible. Using R_g for the molar gas constant, T for the temperature, R for the radius of the droplet, and δ_t for the Tolman length,[1c] we can relate the change in surface excess N_s to the interfacial tension γ via the (curvature corrected) Gibbs equation:[1b,c]

$$\frac{\delta\gamma(1 - 2^{\delta_t}/_R)}{\delta(\ln(c))} = -2R_gTN_s \qquad (1)$$

The Tolman length is a measure of the surface thickness and is on the order of 1−5 Å. Assuming a unitary activity constant we find that the correction needed for high curvature (δ_t/R) is negligible. Taking N_s from our data we can derive the change in interfacial tension ($\Delta\gamma$) as a function of bulk concentration by integrating $-2R_gTN_s/c$. The result is that the derived interfacial tension (Figure 2B, blue squares) changes by only −5 mN/m when the SDS bulk concentration is varied over 3 orders of magnitude. Corresponding data for the equivalent planar interface shows a significantly larger drop in interfacial tension of −42 mN/m (Figure 2B, red circles).

Thus, although on a planar interface the interfacial tension drops dramatically due to surfactant action, this clearly does not happen on the corresponding nanoscopic droplet interface. Our data are in agreement with ζ-potential measurements and our findings would explain the discrepancy between calculated and measured Ostwald ripening rates (see the SI). Additional experiments need to be performed, however, on more surfactants and oils, using cosurfactants and higher concentrations of electrolyte to uncover the mechanism behind droplet stabilization, which is very different for kinetically stable (nano)emulsions and thermodynamically stable microemulsions, in which the surface tension is reduced by orders of magnitude.

Acknowledgment. This work is part of the research program of the Max Planck Society. We acknowledge the Alexander von Humboldt Foundation, the German Science Foundation (Nr. 560398), and the European Research Council (Nr. 240556).

Supporting Information Available: Supporting text regarding materials and methods (p S1), droplet stability (p S2, Figure S1), droplet size distribution and Ostwald ripening (pp S4−S5, Figure S2), S−O ppp spectra (p S6, Figure S3), spectra in the C−H stretching region (p S7, Figure S4), fitting and the modified Langmuir model (pp S8−S11, Figure S6), and the equation for fitting ζ-potential data (p S11). This material is available free of charge via the Internet at http://pubs.acs.org.

References

(1) (a) Hunter, R. J. *Foundations of Colloid Science*; Oxford University Press: Oxford, 2002. (b) Adamson, A. W.; Gast, A. P. *Physical chemistry of surfaces*; Wiley-interscience: New York, 1997. (c) Tolman, R. C. *J. Chem. Phys.* **1949**, *17*, 333–337. (d) Hunter, R. J. *Zeta potential in Colloid Science*; Academic Press: London, 1986.
(2) (a) Langmuir, I. *Chem. Rev.* **1933**, *13*, 147–191. (b) Messmer, M. C.; Conboy, J. C.; Richmond, G. L. *J. Am. Chem. Soc.* **1995**, *117*, 8039–8040. (c) Conboy, J. C.; Messmer, M. C.; Richmond, G. L *J. Phys. Chem.* **1996**, *100*, 7617–7622. (d) Conboy, J. C.; Messmer, M. C.; Richmond, G. L. *Langmuir* **1998**, *14*, 6722–6727. (e) Staples, E.; Penfold, J.; Tucker, I. J. *J. Phys. Chem. B* **2000**, *104*, 606–614. (f) Richmond, G. L *Chem. Rev.* **2002**, *102*, 2693–2724. (g) Knock, M. M.; Bell, G. R.; Hill, E. K; Turner, H. J.; Bain, C. D. *J. Phys. Chem. B* **2003**, *107*, 10801–10814. (h) Schlossman, M. L.; Tikhonov, A. M. *Annu. Rev. Phys. Chem.* **2008**, *59*, 153–177.
(3) Rehfeld, S. *J. Phys. Chem.* **1967**, *71*, 738–745.
(4) (a) Wang, H. F.; Yan, E. C. Y.; Borguet, E.; Eisenthal, K. B. *Chem. Phys. Lett.* **1996**, *259*, 15–20. (b) Wang, H. F.; Yan, E. C. Y.; Liu, Y.; Eisenthal, K. B. *J. Phys. Chem. B* **1998**, *102*, 4446–4450.
(5) (a) Dadap, J. I.; Shan, J.; Eisenthal, K. B.; Heinz, T. F. *Phys. Rev. Lett.* **1999**, *83*, 4045–4048. (b) Wang, H. F.; Troxler, T.; Yeh, A.; Dai, H. *Langmuir* **2000**, *16*, 2475–2481. (c) Yang, N.; Angerer, W. E.; Yodh, A. G. *Phys. Rev. Lett.* **2001**, *87*, 103902-1-4. (d) Eisenthal, K. B. *Chem. Rev.* **2006**, *106*, 1462–1477.
(6) (a) Roke, S.; Roeterdink, W. G.; Wijnhoven, J. E. G. J.; Petukhov, A. V.; Kleyn, A. W.; Bonn, M. *Phys. Rev. Lett.* **2003**, *91*, 258302-1-4. (b) Roke, S. *Chem. Phys. Chem.* **2009**, *10*, 1380–1388.
(7) Sugiharto, A. B.; Johnson, C. M.; de Aguiar, H. B.; Aloatti, L.; Roke, S. *Appl. Phys. B: Laser Opt.* **2008**, *91*, 315–318.
(8) (a) Guyot-Sionnest, P.; Hunt, J. H.; Shen, Y. R. *Phys. Rev. Lett.* **1987**, *59*, 1597–1600. (b) Harris, A. L.; Chidsey, C.; Levinos, N.; Loiacona, D. *Chem. Phys. Lett.* **1987**, *141*, 350–356. (c) Bain, C. D. *J. Chem. Soc., Faraday Trans.* **1995**, *91*, 1281–1296. (d) Shen, Y. R. *Nature* **1989**, *337*, 519–525.
(9) (a) Johnson, C. M.; Tyrode, E. *Phys. Chem. Chem. Phys.* **2005**, *7*, 2635–2641. (b) Hore, D.; Beaman, D.; Richmond, G. L. *J. Am. Chem. Soc.* **2005**, *127*, 9356–3957. (c) de Beer, A. G. F.; Roke, S. *Phys. Rev. B* **2007**, *75*, 245438-1-8.

JA9095158